

## Structural Texture Induced in SnSe Thermoelectric Compound via Open Die Pressing

C. Fanciulli<sup>1,\*</sup>, M. Coduri<sup>1</sup>, S. Boldrini<sup>2</sup>, H. Abedi<sup>1</sup>, C. Tomasi<sup>1</sup>, A. Famengo<sup>2</sup>,  
A. Ferrario<sup>2</sup>, M. Fabrizio<sup>2</sup>, and F. Passaretti<sup>1</sup>

<sup>1</sup>Italian National Research Council—Institute of Condensed Matter Chemistry and Technologies for Energy, Lecco Unit,  
Corso Promessi Sposi, 29, 23900, Lecco, Italy

<sup>2</sup>Italian National Research Council—Institute of Condensed Matter Chemistry and Technologies for Energy, Padova Unit,  
Corso Stati Uniti, 4, 35127, Padova, Italy

Outstanding ZT values registered on single crystals recently renewed the interest of thermoelectric community for SeSn compound. Owing to the strong anisotropy of the phenomenon, so far only single crystals proved to be the suitable for its application. Here we present the production and the characterization of bulk polycrystalline materials processed by open die pressing, aimed at reducing the gap with single crystal materials by taking advantage from the highly texture degree derived by the processing and by the improved phonon scattering promoted by grain boundaries. The resulting bulks display good compaction, improved mechanical properties and strong texture of the phase. Structural and morphological analyses confirmed the successful orientation according to the (400) cleavage plane. The structural transition responsible for the ultra-low thermal conductivity has been investigated and possible irreversible effects on the starting phase due to thermal cycling have been evaluated. Preliminary measurements of thermal conductivity are reported.

**Keywords:** Thermoelectric Material, Open Die Pressing, Texturing Analyses, Structural Refinement.

### 1. INTRODUCTION

The search for the enhancement of the adimensional figure of merit, ZT, for thermoelectric materials has always been one of the main focuses of the thermoelectric community. Looking for a large scale diffusion of thermoelectric technology in the field of waste heat recovery, the improvement of ZT means to extend the range of applications appealing to thermoelectric technology, making it more competitive as respect to other solutions available.

In the framework of bulk materials, the outstanding results reported in literature for low dimensional/nanostructured materials, still don't find an equivalent because of the difficulties met in reproducing nanostructures effective to produce similar improvements into the material and, in most of the cases, to ensure the stability of the results at the operating temperatures considered for each class of material.

One way already explored to develop improved bulk materials is based on the capability to take advantage of the natural anisotropy of some materials trying to produce

samples highly textured to create a preferred direction in the samples produced. This kind of approach has been reported for chalcogenides compounds showing interesting results in term of ZT for both *p* and *n* compounds.<sup>2–5</sup> One of the main strategies proposed in literature is to induce a grain growth during sintering along a preferential orientation, under the action of a strong driving force. The degree of texture observed is a function of the technique used, resulting by the superimposition of different processing parameters like time, temperature and pressure.

In the recent works by Zhao et al.<sup>1,6</sup> unexpectedly high ZT value for SnSe compound has been reported. In particular, the authors showed a strong dependence of material properties on the crystallographic orientation considered for the thermoelectric parameters characterization: in the best configuration ZT up to 2.6 was observed. Looking at the available literature reports on the same system, similar results appear hard to be reproduced in polycrystalline samples.<sup>7–9</sup> In fact, polycrystalline materials displayed a less stable chemical behavior at high temperature showing a low Sn segregation, as reported in Ref. [7]: an anomalous behavior of electrical resistivity has been associated

\* Author to whom correspondence should be addressed.

to this change with respect to the single crystal. The key to obtain the performances of the material presented by Zhao et al. seems to resemble the anisotropic nature of the 'single crystal': this form allows to select a specific orientation being sure to neglect the negative effects associated to the others.

In this paper we propose to use open die pressing (ODP) technique<sup>4</sup> to prepare polycrystalline samples of SnSe compound. This process has been successfully used to sinter powders of different classes of thermoelectric materials.<sup>4,10,11</sup> The main features of the technique are the rapidity of the process, its easy scalability and the capability to induce strong texturing effects into the final element produced.<sup>4</sup> Using this strategy, we have been able to produce highly textured polycrystalline samples: the high degree of alignment of (*h*00) planes induced by the deformation process, offers the possibility to improve phonon scattering due to the presence of grain boundaries, still saving the strong anisotropy among the full scale sample. The advantage having the polycrystalline material, in addition to the reduction of thermal conductivity of the system, is related to the mechanical properties and to the ease to obtain large scale samples.

In this work SnSe compound has been synthesized, reduced to powder and sintered using ODP process. Diffraction analyses have been performed on powders and sintered material to evaluate the chemical and structural evolution of the material due to the processing. The degree of texturing has been deduced analyzing the data collected. Structural data have been collected up to 600 °C in order to investigate the structural transition and the phase stability at high temperature.

Thermal conductivity along different directions has been measured obtaining a value lower than the one reported in literature.<sup>1,6</sup> Thermoelectric properties are still under investigation, but preliminary tests confirm the strong anisotropy in the properties measured following different orientations of the material.

## 2. EXPERIMENTAL DETAILS

SnSe compound has been prepared following the route suggested by Zhao et al.:<sup>1</sup> shots of pure elements (tin purity 99.99+%, selenium purity 99.999%) were mixed in a quartz vial sealed in low argon depression. The presence of the gas helps in preventing possible oxidation of the material during the process even in case of leakage in the vial. The material is heated up to 950 °C using 100 °C/hr as heating rate. According to the phase diagram, the liquids of the two elements are not completely miscible even at high temperature, so the samples were left at 950 °C for 8 hours promoting the homogeneous inter-diffusion of the precursors in the liquid state. The material was cooled following the natural profile of the furnace.

The ingots were ground in mortar and refined using ball milling (Fritsch Pulverisette 4 planetary ball mill) for

90 min at 225 rpm in order to obtain powders to be used for open die pressing sintering.

The materials used for ODP processing were iron tube internally treated with a thin boron nitride layer as metallic sheath for material containment and opportunely shaped Al plugs used to close the two ends of the tube. Powders were manually pressed into the tube and stocked to reach a sufficient compaction into a glovebox under Ar atmosphere. The plugs are designed to allow the outflow of the Ar gas during the process: this solution allowed to prevent oxidation of the material during the pre-heating and, at the same time, to avoid gas residuals during the sintering process, to reach the target of a full dense material. Sintering process were performed at 465 °C for 10 minutes and naturally cooled down. The plastic deformation applied to the composite billets goes from 60% up to 72% depending on the final thickness of the sample. No sticking was observed between thermoelectric and sheath materials.

X-ray diffraction (XRD) structural analyses were performed using PANalytical X'Pert Pro diffractometer with Bragg-Brentano geometry and Cu K $\alpha$  radiation. The system is equipped with thermal chambers used for the analyses up to 600 °C. A detailed structural investigation (quantitative phase analysis, lattice parameters, atomic positions and texture) was performed by Rietveld refinement of the XRD patterns using GSAS software.<sup>12</sup> Rietveld refinements of textured specimens were carried out employing the preferred orientation correction implemented in the GSAS software, based on spherical harmonic functions. From the coefficients of the harmonic functions (which depend on the sample orientation and reflections) a texture index (*ti*) was calculated, which estimates the magnitude of the texture effect. For an ideally oriented powder sample, *ti* is equal to 1, while it diverges to infinite in the limit of a single crystal specimen. It then turns out that the greater *ti*, the larger the texture.

Thermo-gravimetric analyses have been performed using TA instruments SDT Q600 to verify the thermal stability of the compound in the range of temperature set for the characterizations.

The microstructures of the materials as cast and after sintering have been investigated using scanning electron microscope (SEM LEO 1430) equipped with electron probe microanalysis (EPMA Oxford INCA x-sight 7353).

The samples for the thermoelectric properties characterization have been cut by electro-erosion: disks up to 12.5 mm in diameter were prepared from the sample large surface and used for laser flash analyses. For electrical properties (Seebeck and electrical conductivity), rectangular pellets were cut both in the orthogonal and parallel direction with respect to the disk thickness.

Thermal diffusivity of the samples has been measured using Netzsch Laser Flash facility LFA 457: the specific heat of the material, needed to deduce the thermal conductivity, has been measured both by calorimetric and

laser flash ways using TA Instruments DSC Q100 and Netzsch LFA 457 respectively.

### 3. RESULTS AND DISCUSSION

In Figure 1 a picture of the as cast ingot of SnSe is reported: the surface of the ingot suggests a strong tendency to crystalize in a regular shape. The material expands during solidification, so the ingot doesn't display the typical structures associated to the alloys solidification. The ingot has been segmented to investigate the microstructure and evaluate the solidification behavior of the alloy. The microstructure shows a strong tendency to form organized crystals disposed in layers: optical micrographs acquired using polarized light show the presence of layered structures packed to form domains randomly oriented. These elements suggest a strong tendency to grain growth in preferred orientation. In Figure 2 the details of the microstructure of the ingot are reported. The structure shows the tendency to a layered growth with the planes regularly organized in packages (Fig. 2(a)). The substructure of the packed layers has a fine structure with the thickness of the layers below  $1\ \mu\text{m}$ . The packages are randomly oriented into the ingot, so an alternation of flat-planar structures and layered blocks elements has been found. Looking deeper into the layers (Fig. 2(b)), the system displays a layered sub-structure for each layer. Energy-dispersive spectroscopy (EDS) analyses do not point out any relevant difference in composition or character of the layers: the analyses performed confirmed the material composition among different areas of the sample. A deep investigation of the layered structure indicates a morphological nature of the layers, not characterized by a significant difference in terms of chemical composition. This characteristic structure can justify the strong tendency of the material to cleave instead of breaking. The material is highly fragile but during the milling process of the bulk the powder obtained has a flakes-like structure instead of particle like one.



**Figure 1.** SnSe ingot as synthesized extracted from the quartz vial. The strong tendency to crystal growth is visible at the surface of the sample.

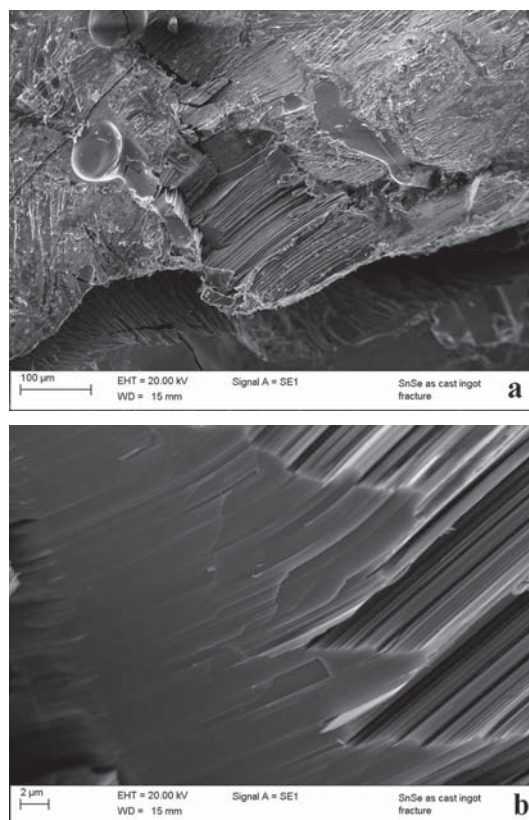


**Figure 2.** Microstructural details of the material as cast. (a) The layered structure of the material, responsible for its easy cleavage, is here visible in the fracture of the ingot. (b) Increasing the magnification a layered organization of each layer appears visible.

The powders obtained are used to produce a sintered bulk by ODP technique: an example of the resulting sample is reported in Figure 3. The bulks produced reach large sizes being the typical shape  $25 \times 45\ \text{mm}^2$  and thickness between 3 and 10 mm. The samples reached a density of

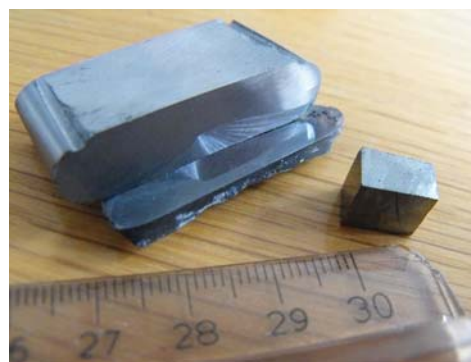


**Figure 3.** ODP sintered bulk of SnSe. The sample on the right has been cut to perform thermoelectric characterizations. Slices of the material were cut in different directions for structural investigations.

6.089 g/cm<sup>3</sup> corresponding to 98.5% of theoretical value.<sup>9</sup> The sintered bulks are no more brittle: the mechanical behavior of the material is improved by the processing and samples were easily cut to investigate the properties in the different orientations with respect to the pressing direction. The microstructural investigation performed on the sintered samples confirms the high density reached but shows the presence of porosity especially closer to the surface of the bulk: this effect could be due to an interaction of the material with the BN used to prevent inter-diffusion between the iron of the external tube and the thermoelectric powders during the ODP process. The fracture analysis reported in Figure 4 shows the presence of a layered structure oriented parallel to the surface of the sample. The microstructure of the ODP samples appears to be finer than the one observed in the ingot: a strong anisotropy in the shape of the elements is still dominating the scenario, but in this case a large number of small fractured particles are distributed between the different stacks of planes. The analyses indicate a reduced growth of the starting particles and a promoted alignment of the planes due to the action of the compression. The thickness of the plane structures

is similar in the as-cast and sintered material, but in the second one a lot of fine particles dispersed are visible. This aspect comes from the starting powders, unable to growth due to the reduced time and temperature used for the sintering process.

The experimental XRD patterns collected on SnSe samples, in powder and ODP sintered bulk forms, are reported as black and red lines respectively in Figure 5. The calculated profile expected from a reference material with no texture is plotted as a green line. The pattern indicates a pure SnSe phase without secondary phases or precursors residuals. The Rietveld refinement of the patterns has been performed to calculate lattice parameters of the material: the resulting *Pnma* structure matches well the one reported in literature;<sup>1,14,15</sup> the lattice parameters obtained are  $a = 1.149$  nm,  $b = 0.444$  nm,  $c = 0.415$  nm. Two conclusions can be readily drawn: given the reflection geometry of the XRD experiment, the higher intensity of the (400) reflection observed in the experimental pattern indicates that (*h*00) reflections are preferentially distributed on the plane perpendicular to the incoming beam, i.e., parallel to the surface of the flat sample. Even though crushed into powder, the material still exhibits the same texture effect, though to a lower extent. This last result can be explained considering that the powders are mostly obtained by cleaving along the original planes instead of breaking randomly the structure, producing a preferred orientation in the powder samples.

Whereas the estimate of the texture magnitude performed on the basis of the intensity extracted by single peak fitting procedure may be strongly affected by peak overlap, as it is in the case of the present SnSe compound, the advantage of employing spherical harmonic functions through Rietveld refinements lies in that the corresponding coefficients are extracted from the analysis of the full XRD pattern.

The best fit from Rietveld refinements on the material, both in powdered and bulk ODP sintered form, are reported in Figures 6(b and d) respectively. The corresponding values for texture index are  $ti \sim 4$  for the powder and  $ti \sim 14$  for the bulk specimen. The good quality of the fit is made evident by the fact that calculated intensities (red solid lines) match very well the experimental patterns (empty circles), thus supporting the reliability of the *ti* values extracted through the refinement. Most importantly, exactly the same *ti* values were found for another specimen produced from another batch of reactants, thus supporting the reproducibility of the material processing procedure as well as the characteristic of the materials produced.

The fit obtained for the two patterns already considered without applying the correction for preferred orientation are shown in Figures 6(a and c). Whereas the most of the peaks are completely misshaped in the case of the bulk specimen, this effect much reduces in the case of the powder, where only the (400) reflection seems to be

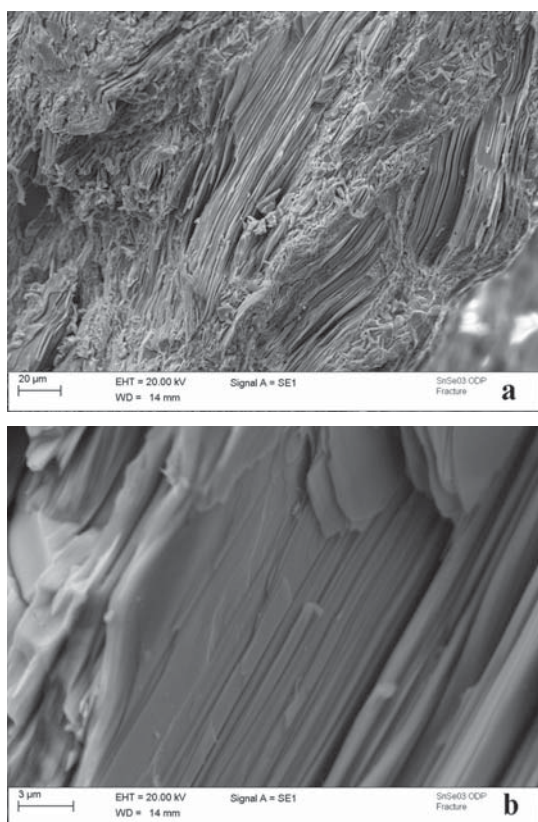


**Figure 4.** The microstructure of the sintered bulk: the material preserves the layered structure (a) but with a reduced size of the constituents. The observations display a preferred direction for the layers alignment into the material (b).

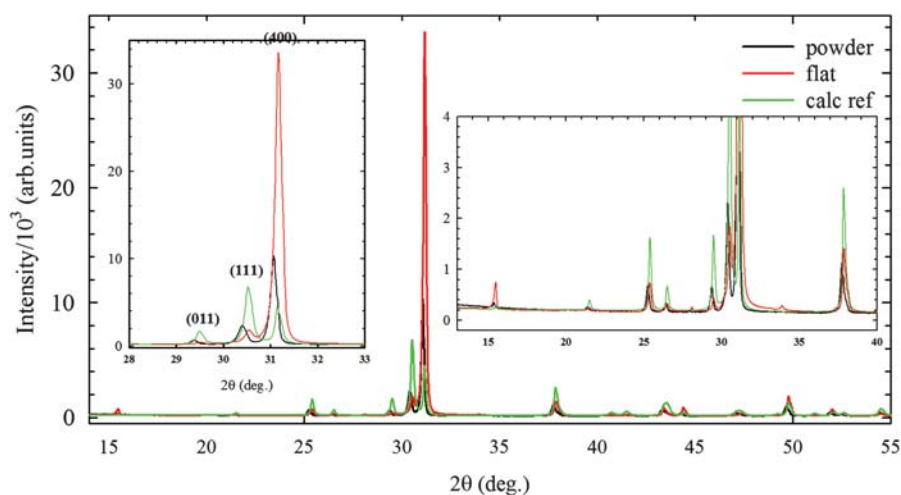


**Figure 5.** The experimental patterns collected on SnSe samples, in powder (black line) and ODP sintered bulk (red line) forms. The green line represents the calculated profile expected from a reference material with no texture. In the insets, details of the patterns close to the (400) reflection are reported to underline the effects related to texture observed in the ODP sample.

completely at odds with the experimental profile. This finding might support the preferential cleavage of the only (400) planes.

By increasing temperature, SnSe is known to reversibly transform from *Pnma* to the high temperature *Cmcm* phase.<sup>1,14,15</sup> The transformation is accompanied by a change of setting, so that the high temperature lattice parameters ( $d'$ ) are related to the low temperature ones ( $d$ ) in the form:  $a' = c$ ,  $b' = a$ ,  $c' = b$ . The results reported

in the following are referred to the low temperature setting. The evolution of the lattice parameters is reported in Figures 7(a) ( $a$ -axis) and 7(b) ( $b$  and  $c$  axes). Although the lattice parameter  $a$  grows roughly linearly with temperature, the same does not apply to  $b$  and  $c$  axes, which tend to converge at high temperature. The corresponding orthorhombic distortion, defined as  $m = 2(a - b/a + b)$ , is reported in Figure 7(c). A similar trend can be observed for the  $z$  coordinate of the Sn site, Figure 7(d). The Sn site

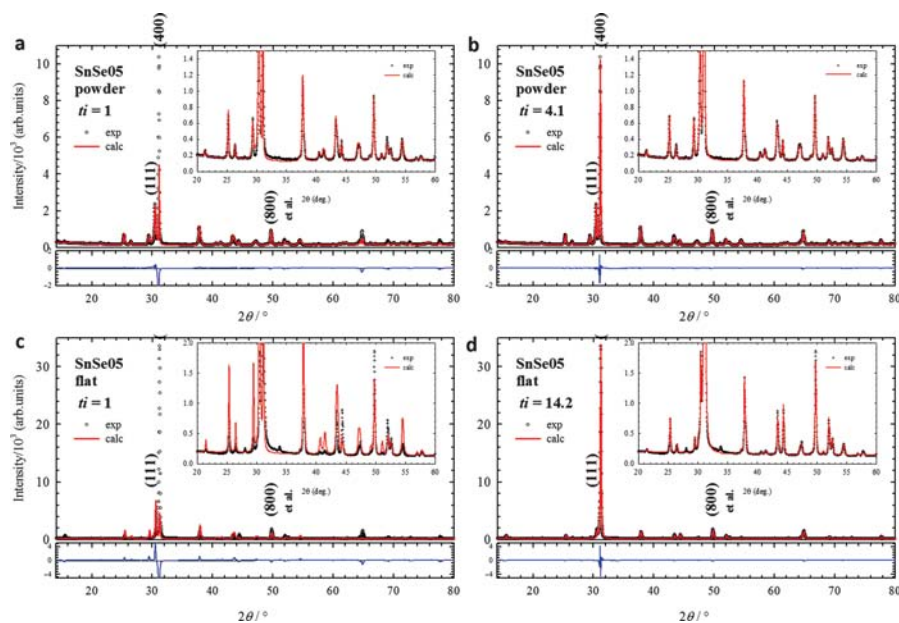


**Figure 6.** Rietveld refinements of experimental patterns for powder (a, b) and sintered bulk (c, d) samples. For the cases 6(a and c) the refinement are performed neglecting the texture index (fixed to 1) contribution. In cases 6(b and d) the texture index is considered a refinement parameter and the values obtained are reported: the texture observed after ODP sintering is 3.5 times greater than the one resulting for the starting powders.

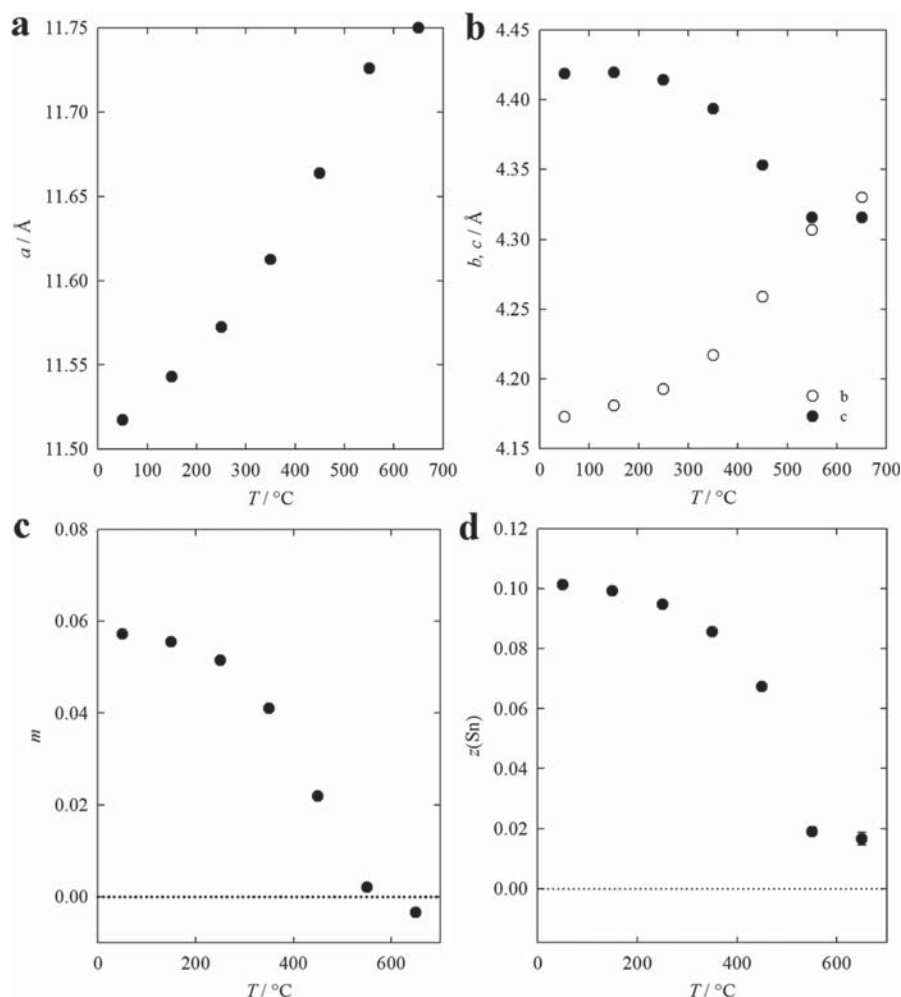


**Figure 7.** Lattice parameters plotted as a function of temperature. The four plots describe the evolution of the structure parameters increasing the temperature: (a) the  $a$ -axis; (b) the  $b$ - and  $c$ -axes; (c) the orthorhombic distortion parameter  $m$  and (d) the  $z$  coordinate of Sn atom position. All the characteristics show the structural transition taking place close to 550 °C.

is a good reference due to the strong contrast X-rays have in its respect.

Although the evolution of the lattice parameters with temperature resembles that of an orthorhombic to tetragonal transformation, this phenomenon is only a side effect of the crystallography of the transformation, which instead leads to an orthorhombic  $Cmcm$  phase and it is driven by the shift of two atomic coordinate, namely  $z(\text{Sn})$  and  $x(\text{Se})$ , towards special positions, i.e., 0 and 0.5 respectively. As a consequence, extinction rules changes and some reflections are expected to vanish, as it is the case of the (011) plane reported in Figure 8: here the peak disappears increasing the temperature above the one corresponding to the structural transition. The fail of the expected vanishing of  $z(\text{Sn})$  might be related to the strong correlation which occurs between the refined values of atomic coordinates and preferred orientation coefficients.

The evolution of experimental patterns, of the derived atomic coordinates and of the lattice parameters is consistent with a transformation from  $Pnma$  to  $Cmcm$  occurring close to 550 °C.

The specific heat of the material as a function of temperature up to 600 °C is reported in Figure 9: the values obtained are comparable to the ones already reported in literature for the pure material.<sup>1,16,17</sup> No anisotropic effects are expected for the  $C_p$  of the material: this can be confirmed by the similarity of the results obtained using calorimetric analyses performed on not textured samples. The curve of  $C_p$  displays a peak, indicating the presence of a transformation of the material, at 500 °C: the temperature is in agreement with the one deduced for the structural transformation by XRD analyses. In fact, the discrepancy can be explained considering the different techniques used: XRD analyses show the end of the structural

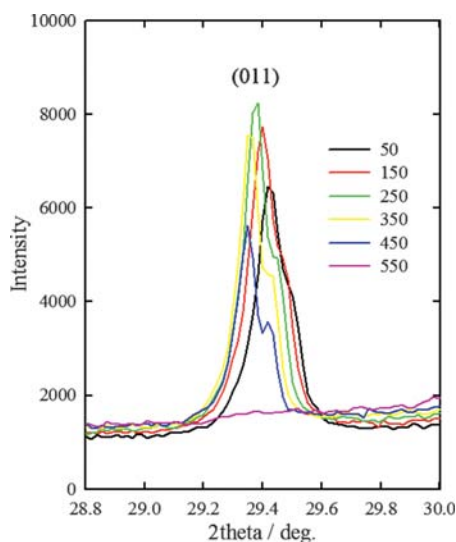


**Figure 8.** The peak corresponding to the (011) reflection plotted at different temperatures. The structural transition causes this reflection to vanish at high temperature.

transition, happening before 550 °C, while calorimetric analyses display the transition itself, taking place at 500 °C and already ended at 550 °C.

The thermal conductivity of the sintered material as a function of temperature is also reported in Figure 9. The data for the different orientations of the sample are still not available but these preliminary results for  $\kappa$  display behavior with the temperature and values close to the ones reported by Zhao et al.<sup>1</sup> along the *b*- and *c*-axes of the material. This result seems to suggest that a structural refinement, corresponding to increasing the number of grain boundaries, poorly contributes to the reduction of thermal conductivity of the material. This could be explained looking at the deep sub-structure of the material as cast presented in Figure 2(b): the layered growth of the material seems to be responsible for the reduced effect of

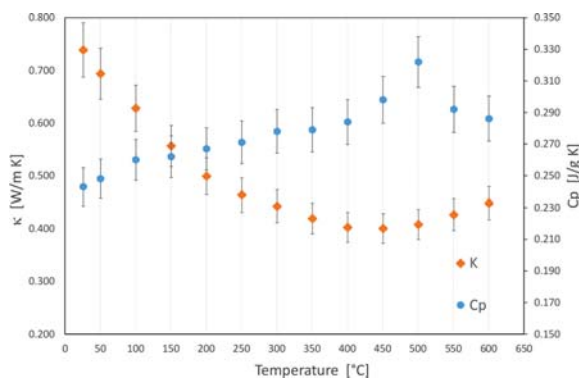


**Figure 9.** Specific heat and thermal conductivity measured by laser flash method in the range of temperature RT–600 °C. The peak visible at 500 °C is associated to the structural transition of the material.

grain boundaries on thermal conductivity, acting efficiently in phonon scattering.

#### 4. CONCLUSIONS

ODP is here proposed as a method for fast sintering polycrystalline SnSe resembling the strong structural anisotropy typical of single crystals, likely at the basis of the outstanding physical properties reported by Zhao et al.<sup>1</sup>

As cast SnSe ingots were crushed and ball-milled into powder, then pressed at 465 °C to get a body with density as large as 98.5% of the theoretical value. The resulting material shows promising morphological and structural characteristics.

The microstructural investigation through electron microscopy revealed that that layered morphology with the planes regularly organized in packages is retained across the ODP process. The finer microstructure observed in processed samples contributes to reduce the strong cleavage effect observed in the starting material. The comparison between analyses performed on differently oriented surfaces of the samples showed the strong alignment of the grains obtained after ODP processing.

The material was full SnSe with no fingerprint of secondary phases. The lattice parameters were consistent with results reported in the literature and the same applies to the high temperature transformation from *Pnma* to *Cmcm* phases, which was probed to occur close to 550 °C by the evolution of the Sn *z*-coordinate towards a special position characteristic of the *Cmcm* phase. The transition temperature was also confirmed by specific heat measurement.

Both the bulk and the powdered materials showed strong texture consistent with the preferential cleavage on (400) planes, this effect being much more remarkable for the ODP processed specimens.

Thermal conductivity measurements reproduced the results already reported for single crystals suggesting a minor contribution of grain boundaries to the phonon scattering in this system. Deeper analyses have to be performed to confirm these considerations and the other thermoelectric parameters have to be characterized in order to determine the final ZT of the polycrystalline samples obtained using ODP process.

**Acknowledgments:** The authors want to thank Mr. Enrico Bassani for his contribution to the samples preparation and Mr. Giordano Carcano for the support in XRD experiments.

#### References and Notes

1. L.-D. Zhao, S.-H. Lo, Y. Zhang, H. Sun, G. Tan, C. Uher, C. Wolverton, V. P. Dravid, and M. G. Kanatzidis, *Nature* 508, 373 (2014).
2. X. Yan, B. Poudel, Y. Ma, W. S. Liu, G. Joshi, H. Wang, Y. Lan, D. Wang, G. Chen, and Z. F. Ren, *Nano Lett.* 10, 3373 (2010).

3. D. Vasilevskiy, J.-M. Simard, F. Bélanger, F. Bernier, S. Turenne, and J. L'Ecuyer, *21th International Conference on Thermoelectrics Proceedings*, IEEE, Long Beach CA (2002), p. 24.
4. S. Ceresara, C. Fanciulli, F. Passaretti, and D. Vasilevskiy, *J. Electron. Mater.* 42, 1529 (2013).
5. J. Yang, R. Chen, X. Fan, W. Zhu, S. Bao, and X. Duan, *J. Alloy. Compd.* 429, 156 (2007).
6. L.-D. Zhao, G. Tan, S. Han, J. He, Y. Pei, H. Chi, H. Wang, S. Gong, H. Xu, V. P. Dravid, C. Uher, G. J. Snyder, C. Wolverton, and M. G. Kanatzidis, *Science* 351, 141 (2016).
7. S. Sassi, C. Candolfi, J.-B. Vaney, V. Ohorodniichuk, P. Masschelein, A. Dauscher, and B. Lenoir, *Appl. Phys. Lett.* 104, 212105 (2014).
8. S. Sassi, C. Candolfi, J.-B. Vaney, V. Ohorodniichuk, P. Masschelein, A. Dauscher, and B. Lenoir, *Mater. Today Proc.* 2, 690 (2015).
9. C.-L. Chen, H. Wang, Y.-Y. Chen, T. Day, and G. J. Snyder, *J. Mater. Chem. A* 2, 11171 (2014).
10. C. Fanciulli, S. Battiston, S. Boldrini, E. Villa, A. Famengo, S. Fiameni, M. Fabrizio, and F. Passaretti, *Mater. Today Proc.* 2, 566 (2015).
11. A. Castellero, C. Fanciulli, R. Carlini, G. Fiore, P. Mele, F. Passaretti, and M. Baricco, *J. Alloy. Compd.* 653, 54 (2015).
12. A. C. Larson and R. B. Von Dreele, General Structure Analysis System (GSAS), National Laboratory Report, Los Alamos (2000), pp. 86–748.
13. S. Boldrini, A. Famengo, F. Montagner, S. Battiston, S. Fiameni, M. Fabrizio, and S. Barison, *J. Electron. Mater.* 42, 1319 (2013).
14. T. Chattopadhyay, J. Pannetier, and H. G. Von Schnering, *J. Phys. Chem. Solids* 47, 879 (1986).
15. H. Weidemeier and H. G. von Schnering, *Z. Kristallogr.* 148, 295 (1978).
16. H. Wiedemeier, G. Pultz, U. Gaur, and B. Wunderlich, *Thermochim. Acta* 43, 297 (1981).
17. L. Baldè, B. Legendre, C. Souleau, P. Khodadad, and J. R. Didry, *J. Less-Common Met.* 80, 45 (1981).

Received: 5 April 2016. Accepted: 26 May 2016.